

Intermittent chaotic chimeras for coupled rotators

Simona Olmi,^{1,2,*} Erik A. Martens,^{3,4,5,†} Shashi Thutupalli,^{6,7,‡} and Alessandro Torcini^{1,2,8,9,§}

¹*Consiglio Nazionale delle Ricerche, Istituto dei Sistemi Complessi, Via Madonna del Piano 10, I-50019 Sesto Fiorentino, Florence, Italy*

²*INFN Sezione Firenze, Via Sansone 1, I-50019 Sesto Fiorentino, Florence, Italy*

³*Department of Biomedical Sciences, University of Copenhagen, Blegdamsvej 3, 2200 Copenhagen, Denmark*

⁴*Department of Mathematical Sciences, University of Copenhagen, Universitetsparken 5, 2100 Copenhagen, Denmark*

⁵*Group of Biophysics and Evolutionary Dynamics, Max Planck Institute for Dynamics and Self-Organization, 37077 Göttingen, Lower Saxony, Germany*

⁶*Department of Physics, Princeton University, Princeton, New Jersey 08544, USA*

⁷*Department of Mechanical and Aerospace Engineering, Princeton University, Princeton, New Jersey 08544, USA*

⁸*Aix-Marseille Université, Inserm, INMED UMR 901 and Institut de Neurosciences des Systèmes UMR 1106, 13000 Marseille, France*

⁹*Aix-Marseille Université, Université de Toulon, CNRS, CPT, UMR 7332, 13288 Marseille, France*

(Received 6 May 2015; revised manuscript received 14 August 2015; published 9 September 2015)

Two symmetrically coupled populations of N oscillators with inertia m display chaotic solutions with broken symmetry similar to experimental observations with mechanical pendulums. In particular, we report evidence of intermittent chaotic chimeras, where one population is synchronized and the other jumps erratically between laminar and turbulent phases. These states have finite lifetimes diverging as a power law with N and m . Lyapunov analyses reveal chaotic properties in quantitative agreement with theoretical predictions for globally coupled dissipative systems.

DOI: [10.1103/PhysRevE.92.030901](https://doi.org/10.1103/PhysRevE.92.030901)

PACS number(s): 05.45.Xt, 05.45.Jn, 89.75.Fb

Introduction. Chimera states are remarkable dynamical states emerging in populations of coupled identical oscillators, where the population splits into two parts: one synchronized and the other composed of incoherently oscillating elements [1]. These states were initially discovered in chains of nonlocally coupled oscillators, however they can equally emerge in models of globally coupled populations [1–3]. Chimeras have been observed in a repertoire of different models [2–9] and in various experimental settings, including mechanical [10,11], (electro)chemical [12,13], and lasing systems [14], among others. Usually, the incoherent oscillators give rise to regular macroscopic dynamics that are either stationary, periodic (so-called breathing chimera), or even quasiperiodic [3,7]. Only recently have spatiotemporally chaotic chimeras been numerically identified in rings of coupled oscillators [15–18]. However, a detailed characterization of the dynamical properties of these states has been reported only for phase oscillators with finite-range interactions: In this case chimeras are transient and weakly chaotic [16,19]. More specifically, the lifetimes of these states diverge exponentially with the system size, while their dynamics becomes regular in the thermodynamic limit. In contrast, for globally connected populations, chaotic chimeras have so far only been observed in pulse-coupled oscillators [20] without further analysis.

In this Rapid Communication, we report the existence of various irregular solutions with broken symmetry in an experiment with two mechanically coupled populations of pendulums and analyze in depth a model that reproduces this complex dynamics. Three pertinent examples from the experiment, shown in Figs. 1(a)–1(c), are of particular interest.

The first two examples represent chimeras: In Fig. 1(a) the order parameter of the desynchronized population oscillates quite irregularly, while in Fig. 1(b) it enters a regime of almost periodic oscillations. Figure 1(c) reports a situation where both populations are irregularly oscillating. We introduce a simple model [Eq. (1)] capable of reproducing all these different dynamical behaviors, as it can be appreciated by the simulations reported in Figs. 1(d)–1(f). The model consists of two symmetrically globally coupled populations of N Kuramoto phase oscillators with inertia.

The introduction of inertia allows the oscillators to synchronize via the adaptation of their own frequencies, in analogy with the mechanism observed in certain species of fireflies [21]. The modification of the classical Kuramoto model with the addition of an inertial term leads to first-order synchronization transitions and complex hysteretic phenomena [22–27]. Furthermore, networks of phase coupled oscillators with inertia have recently been employed to investigate self-synchronization in power grids [28–31] and in disordered arrays of Josephson junctions [32]. In the absence of dissipation, Eq. (1) reduces to the Hamiltonian mean-field model, a paradigm of long-range interacting systems [33].

Our analysis will mainly focus on the solution shown in Fig. 1(a), which we term an intermittent chaotic chimera (ICC). This state exhibits turbulent phases interrupted by laminar regimes, analogous to the one reported in Fig. 1(b). The third state shown in Fig. 1(c) is a chaotic two-population (C2P) state; here the erratic dynamics is induced by the evolution of the nonclustered oscillators belonging to both populations. In particular, we show that ICCs are transient states for finite inertia and system size, whose lifetimes diverge as a power law with N and m . Furthermore, in the thermodynamic limit the intermittent oscillations disappear and the turbulent regime prevails over the laminar one. The stability properties of the ICC can be ascribed to the universality class of globally coupled systems [34], which are distinct from those reported for chaotic chimeras in chains of oscillators [19]. This result

*simona.olmi@fi.isc.cnr.it

†erik.martens@sund.ku.dk

‡shashi@princeton.edu

§alessandro.torcini@cnr.it

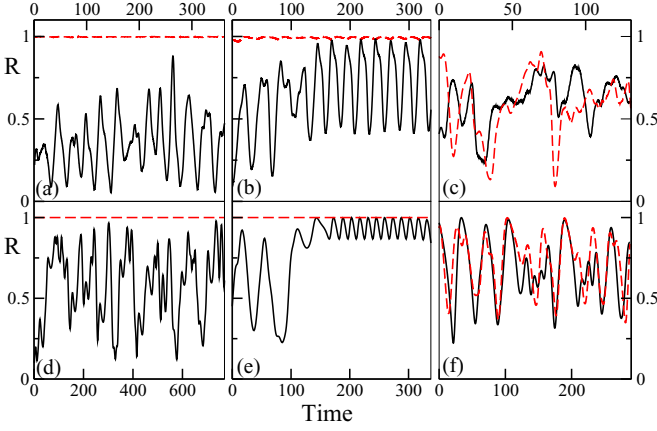


FIG. 1. (Color online) Order parameters $R^{(1)}$ (solid black curve) and $R^{(2)}$ (dashed red curve) for the two coupled populations versus time: (a)–(c) experimental measurements and (d)–(f) numerical simulations of the model (1) with $m = 10$. Initial conditions are (a), (b), (d), and (e) BSCs and (c) and (f) UCs and $N = 15$. The experiments are carried out with (a) and (b) $f = 160$ beats per minute (bpm) and $l = 17$ cm and (c) $f = 184$ bpm and $l = 25$ cm and experimental time is measured in seconds.

clearly illustrates that the stability of chimera states strongly depends on the underlying network topology.

Experimental setup. The setup is shown in Fig. 2 and it is identical to the one described in [10]. The experiment is composed of purely mechanical parts. In particular,

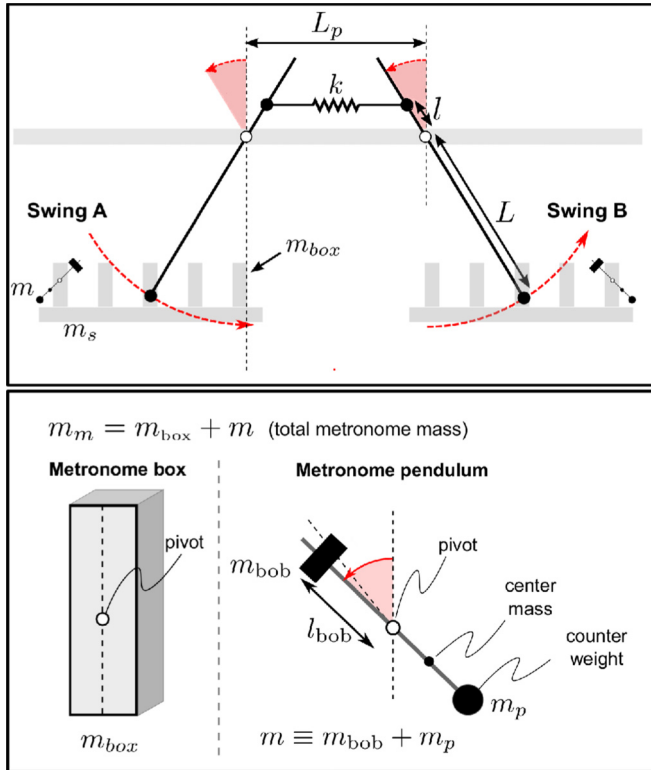


FIG. 2. (Color online) Experimental setup: sketch of the mechanical system studied in [10], composed of two swings (A and B) coupled with a spring mechanism, each of which is loaded with $N = 15$ metronomes.

following [3], two populations of nonlocally coupled metronomes were considered: within each population oscillators were coupled strongly, but they were coupled more weakly to the neighboring population. Metronomes take the role of self-sustained oscillators [35], whose working principle is identical to Huygens's pendulum clocks [36], except that the escapement in the metronome is driven by a spring rather than a mass pulled by gravity. While friction inherent to the mechanical elements attenuates large-amplitude oscillations toward the unperturbed amplitude associated with its unperturbed frequency, small pendulum oscillations are amplified by the spring that drives the metronome via its escapement mechanism. This lends the metronome the characteristics of a self-sustained oscillator [35]. A number $N = 15$ of identical metronomes running with identical frequencies were placed on each of two aluminum swings suspended by four rods. The strong coupling within one population is mediated by the motion of the swing onto which the metronomes are attached. As one increases the common frequency f of the metronomes, more momentum is transferred to the swing, leading to a stronger coupling among the metronomes. A single swing follows a phase transition from a disordered to a synchronized state as the coupling within the population increases [35,37]. The weaker coupling between the two swings is facilitated by a pair of tunable steel springs, attached to the adjacent rods of the opposing swings. The distance of the spring relative to the pivot can be adjusted: This changes the spring lever l and the associated torque, thus effectively tuning the spring coupling strength between the two metronome populations.

The motion of swings and metronomes is visualized by attaching UV fluorescent spots on swings and metronome pendulums and the spot motion is digitally recorded using a digital single-lens reflex photcamera. Subsequently, digital data analysis is used to measure the swing and pendulum motion. The relative motion of the pendulums is reconstructed by subtraction of the swing coordinates. Amplitudes and phases are then obtained via Hilbert transformation of the signal. The phases are used to quantify the level of synchronization for each population by using the order parameters defined in the following. For exhaustive details on the experimental setup and methods, see [10].

Model and methods. We consider a network of two symmetrically coupled populations of N oscillators. The phase $\theta_i^{(\sigma)}$ of the i th oscillator in population $\sigma = 1, 2$ evolves according to the differential equation

$$m\ddot{\theta}_i^{(\sigma)} + \dot{\theta}_i^{(\sigma)} = \Omega + \sum_{\sigma'=1}^2 \frac{K_{\sigma\sigma'}}{N} \sum_{j=1}^N \sin(\theta_j^{(\sigma')} - \theta_i^{(\sigma)} - \gamma), \quad (1)$$

where the oscillators are assumed to be identical with inertia m , natural frequency $\Omega = 1$, and a fixed phase lag $\gamma = \pi - 0.02$. The self-coupling (cross-coupling) among oscillators belonging to the same population (different populations) is defined as $K_{\sigma\sigma} = 0.3$ ($K_{\sigma\sigma'} \equiv K_{\sigma'\sigma} = 0.2$), with $K_{\sigma\sigma} > K_{\sigma\sigma'}$ as in previous studies on chimera states [3,38,39]. We consider two types of initial conditions: (i) broken-symmetry conditions (BSCs), realized by initializing the first (second) population with identical (random) phases and frequencies, which may lead to the emergence of chimera states, and (ii) uniform conditions (UCs) where both populations are initialized with random values and which can result in a CP2 state [40].

The collective evolution of each population will be characterized in terms of the macroscopic fields $\rho^{(\sigma)}(t) = R^{(\sigma)}(t) \exp[i\Psi(t)] = N^{-1} \sum_{j=1}^N \exp[i\theta_j^{(\sigma)}(t)]$. The modulus $R^{(\sigma)}$ is an order parameter for the synchronization transition being one [$\mathcal{O}(N^{-1/2})$] for synchronous (asynchronous) states.

The microscopic stability can be measured in terms of the associated ordered spectrum of the Lyapunov exponents (LEs) $\{\lambda_i\}$, $i = 1, \dots, 4N$, representing the exponential growth rates of infinitesimal perturbations. The dynamics is chaotic whenever the maximal LE $\lambda_M \equiv \lambda_1$ is positive. For the studied model, presenting a constant viscous dissipative term, the spectrum satisfies the following pairing rule [41]: $\lambda_i + \lambda_{4N-i+1} = -1/m$. Therefore, the analysis can be limited to the first $2N$ exponents. The Lyapunov spectrum can be numerically estimated by employing the standard method reported in [42]. This amounts to considering for each LE λ_k , the evolution of a $4N$ -dimensional tangent vector $\mathcal{T}^{(k)} = \{\delta\theta_i^{(1)}, \delta\theta_i^{(2)}, \delta\theta_i^{(1)}, \delta\theta_i^{(2)}\}$, $i = 1, \dots, N$, whose dynamics is ruled by the linearization of Eq. (1):

$$m\delta\dot{\theta}_i^{(\sigma)} + \delta\dot{\theta}_i^{(\sigma)} = \sum_{\sigma'=1}^2 \frac{K_{\sigma\sigma'}}{N} \sum_{j=1}^N A_{ji}^{(\sigma'\sigma)} (\delta\theta_j^{(\sigma')} - \delta\theta_i^{(\sigma)}), \quad (2)$$

where $A_{ji}^{(\sigma'\sigma)} = \cos(\theta_j^{(\sigma')} - \theta_i^{(\sigma)} - \gamma)$. The orbit and the tangent vectors are followed for a time lapse T_s by performing Gram-Schmidt orthonormalization at fixed time intervals Δt , after discarding an initial transient evolution T_t . We have employed $\Delta t = 5$ and $T_t = 5000$; for BSCs we have integrated the system for times $8 \times 10^4 \leq T_s \leq 3 \times 10^5$ with $N = 100, \dots, 800$ and for UCs for times $3 \times 10^4 \leq T_s \leq 1 \times 10^6$ with $N = 100, \dots, 400$. The integrations have been performed with a fourth-order Runge-Kutta scheme with time step 5×10^{-4} .

A characterization of the dynamical evolution on short time scales can be achieved by considering the probability distribution function $P(\Lambda)$ of the finite time LE Λ [43]. The finite time LE is calculated by estimating the exponential growth rate of the magnitude of the maximal tangent vector $\mathcal{T}^{(1)}$ over finite time windows Δt , namely, $\Lambda = \frac{1}{\Delta t} \ln \|\mathcal{T}_i^{(1)}(\Delta t)\|$, where $\|\mathcal{T}^{(1)}(0)\| \equiv 1$. In order to estimate $P(\Lambda)$, we have collected 100 000 data points for each system size, obtained from ten different orbits, each of duration $T_s = 100\,000$ with $\Delta t = 10$.

Intermittent chaotic chimeras. Starting simulations with BSCs at small masses ($m \leq 4$), the system is not chaotic [as shown in Fig. 3(a)] and it displays a multitude of coexisting breathing chimeras [3]. Furthermore, while the synchronous state $R^{(1)} = R^{(2)} \equiv 1$ remains stable also in the presence of inertia ($m > 0$), the stationary chimeras associated with constant order parameters with $R^{(1)} < R^{(2)} \equiv 1$ are no longer observed. For sufficiently large masses, a solution with broken symmetry emerges, where one population is fully synchronized with $R^{(2)} \equiv 1$, while the other population exhibits wide collective irregular oscillations in the order parameter $R^{(1)}(t)$ between zero and one, as shown in Figs. 1(d) and 3(b). These are ICCs and they represent the main subject of this Rapid Communication.

As shown in Fig. 3(b), the erratic oscillations of $R^{(1)}$ are interrupted by laminar phases, where $R^{(1)}$ stays in proximity to

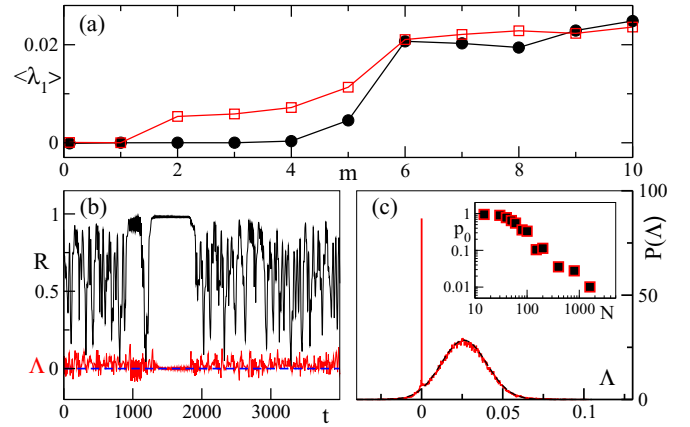


FIG. 3. (Color online) (a) Average maximal LE (λ_1) vs m for $N = 100$: black circles (red squares) refer to BSCs (UCs). (b) Order parameter R (black solid line) and finite time LE Λ (red dashed line) for the chaotic population vs time t for $N = 200$ and $m = 10$. The corresponding $P(\Lambda)$ (solid red line) is shown in (c) with the Gaussian fit (black dashed line). The inset shows the probability p_0 versus N . The values $\langle \lambda_1 \rangle$ are obtained by following each realization for a time span $t = 50\,000$ and by averaging over 100 different initial conditions.

one displaying small oscillations. This regime is characterized by a large part of the oscillators in the chaotic population getting entrained to the synchronous population, apart a few oscillators, which keep oscillating with a common distinct frequency, but with incoherent phases. An analogous regime is also experimentally observed, as reported in Fig. 1(b), however, due to the smaller size of the populations, the amplitude of the oscillations is larger. Furthermore, by estimating the finite time LE Λ , we show that the laminar phases are indeed regular, since they are associated with $\Lambda \simeq 0$ [see Fig. 3(b)]. In particular, the distribution $P(\Lambda)$, reported in Fig. 3(c), reveals a clear peak at $\Lambda = 0$, associated with the laminar regime, superimposed on a seemingly Gaussian distribution. The probability p_0 to observe a laminar phase can be estimated by integrating $P(\Lambda)$ within a narrow interval around $\Lambda = 0$. This probability is reported in the inset of Fig. 3(c) for $10 \leq N \leq 1600$ and it shows a power-law decay with N for sufficiently large system sizes, namely, $N \geq 50$. This is a clear indication that the laminar episodes tend to disappear in the thermodynamic limit.

To characterize the erratic phase, we give an estimate of the average LE $\Lambda^{(*)}$ restricted to this phase. This estimate is obtained by evaluating the maximum of $P(\Lambda)$ with a Gaussian fit to the data, once the channels around $\Lambda = 0$ are removed. The corresponding data, reported in Fig. 4(a) for various N , reveal a clear decay of $\Lambda^{(*)}$ as $1/\ln(N)$. Furthermore, the extrapolated value of $\Lambda^{(*)} \simeq 0.022$ for $N \rightarrow \infty$ is definitely positive, thus indicating that the chaotic state persists in the thermodynamic limit for finite m , contrary to what is usually observed for the Kuramoto model in [19,44]. This logarithmic dependence of the maximal LE λ_M with the system size was previously reported for globally coupled networks in [34], where, for dissipative systems, the authors showed analytically

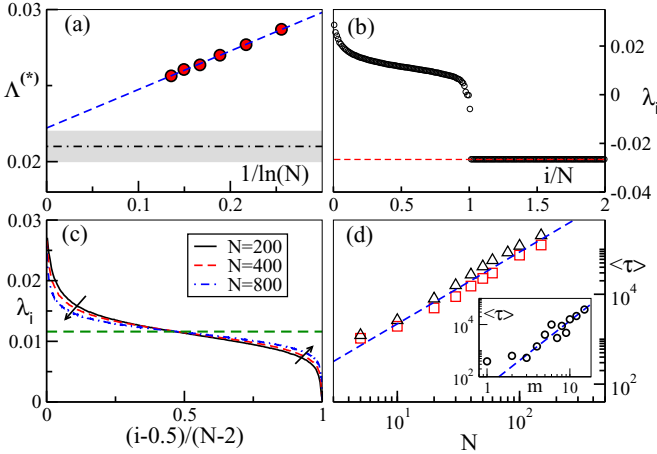


FIG. 4. (Color online) (a) Plot of Λ^* (symbols) versus $1/\ln(N)$ for $50 \leq N \leq 1600$ and the corresponding fit; the dot-dashed black curve with the shaded area denotes $\lambda_M(\infty)$ with its error bar. (b) Lyapunov spectrum for $N = 100$; the dashed red line is $\lambda^{(s)}$. (c) Positive part of the Lyapunov spectra for various sizes, the dashed (green) line is $\lambda^{(c)}$. (d) Average lifetimes $\langle \tau \rangle$ of the ICC vs N for inertia $m = 8$ (red squares) and $m = 10$ (black triangles). The inset shows $\langle \tau \rangle$ vs m for $N = 30$ for ICCs. The blue dashed line in the main panel (inset) refers to a power law with exponent 1.60 (2.50). (a)–(c) The values of $\langle \tau \rangle$ are averaged over 200–3000 different realizations of BSCs and $m = 10$.

that

$$\lambda_M(N) = \lambda^{(c)} + \frac{D}{2} + \frac{a}{\ln(N)} + \mathcal{O}\left(\frac{1}{\ln^2(N)}\right), \quad (3)$$

where $\lambda^{(c)}$ is the mean-field LE obtained by considering an isolated unit of the chaotic population forced by the two fields $\rho^{(1)}$ and $\rho^{(2)}$ and D is the diffusion coefficient associated with the fluctuations of $\lambda^{(c)}$ [34]. In particular, D can be measured by the scaling of the variance of $\ln d(t)$, where $d(t)$ is the modulus of the Lyapunov vector associated with the single forced unity. Namely, for sufficiently long times it is expected that $\langle [\ln d(t) - \lambda^{(c)}t]^2 \rangle \simeq Dt$ with the average $\langle \cdot \rangle$ performed over many realizations. In the present case, we measured $\lambda^{(c)} \simeq 0.0116(5)$ and $D \simeq 0.0180(10)$, thus the expected asymptotic LE should be $\lambda_M(\infty) \simeq 0.021(1)$, which is in good agreement with the previously reported numerical extrapolation as shown in Fig. 4(a). This represents the first quantitative verification of the prediction (3) for a dissipative system with continuous time and in particular for an intermittent dynamics.

A more detailed analysis of the stability of this state can be achieved by estimating the Lyapunov spectra for various system sizes: We observe that the spectrum is composed of a positive part made of $N - 2$ exponents and a negative part composed of N exponents [see Fig. 4(b)]. Two exponents are exactly zero: One is always present for systems with continuous time, while the second arises due to the invariance of Eq. (1) for uniform phase shifts. The negative part of the spectrum is composed of an isolated LE, quantifying the longitudinal stability of the synchronized population, and $N - 1$ identical LEs, which measure the transverse stability of the synchronous solution [45]. The value of this negative plateau in the spectrum coincides with the mean-field LE

$\lambda^{(s)} = -0.0266(5)$ calculated for an isolated oscillator of the synchronized population, as shown in Fig. 4(b).

Furthermore, the central part of the positive spectrum reveals a tendency to flatten towards the mean-field value $\lambda^{(c)}$ associated with the chaotic population for increasing system sizes [see Fig. 4(c) for $N = 200, 400$, and 800], while the largest and smallest positive Lyapunov exponents tend to split from the rest of the spectrum. This scaling of the Lyapunov spectra has been found to be a general property of fully coupled dynamical systems. In particular, the authors in [34,46] have shown that in the thermodynamic limit the spectrum becomes asymptotically flat (thus trivially extensive), but this part is sandwiched between subextensive bands containing typically $\mathcal{O}(\log N)$ exponents scaling as in Eq. (3) with N . We can safely affirm that the chaotic population in the ICC reveals properties that are typical of fully coupled systems, contrasting with the results reported for chaotic chimeras emerging in spatially extended systems [16,19].

Let us now examine if the ICCs are transient states; indeed, we observe for different masses that the chaotic chimeras converge to a regular (nonchaotic) state after a transient time τ . This amounts to the fact that the system remains entrapped in a laminar state, which could be either fully synchronous or a breathing chimera, without returning to the turbulent phase. We have measured the average life times $\langle \tau \rangle$ [47] of the ICCs for two masses, namely, $m = 8$ and 10 , and various system sizes $5 \leq N \leq 150$. These results are displayed in Fig. 4(d). From the figure it is clear that for $N \geq 10$ one has a power-law divergence of the synchronization time with an exponent $\alpha \simeq 1.60(5)$. The divergence of τ is directly related to the vanishing of the laminar phases ($p_0 \rightarrow 0$) observable for $N \rightarrow \infty$. Unfortunately, due to CPU limitations, we cannot explore larger system sizes to verify that this scaling is present over more decades. However, we can safely affirm that these times are not diverging exponentially with N as reported in [16]. This is a further indication that our phenomenon has a different nature, which is deeply related to the topology presently considered. Indeed, exponentially diverging transients for metastable states have usually been reported in the context of spatially extended systems [48], while metastable states with lifetime diverging as $\langle \tau \rangle \propto N^\alpha$ – with $\alpha \simeq 1.7$ – have been reported for the Hamiltonian version of our model [25,49]. Furthermore, we have tested the dependence of $\langle \tau \rangle$ on the mass for one system size, namely, $N = 30$, and we observe that $\langle \tau \rangle$ is diverging also as a power law of m with an exponent 2.50(5) [see the inset of Fig. 4(d)]. It is important to remark that regular chimeras, appearing for $m = 0$, are not transient for this topology, as we have numerically verified.

Chaotic two-population state. With UCs, the system evolves towards chaotic solutions already at smaller masses, namely, $m > 1$, as shown in Fig. 3(a). With these initial conditions the multistability is strongly enhanced and many different coexisting states with broken symmetry are observable, either regular or chaotic. By focusing on the chaotic solutions, the so-called C2P state reported in Figs. 1(c), 1(f), and 5(a), we observe that in all the cases the oscillators of the two populations form a common cluster, characterized by a common average frequency, plus a certain number of oscillators with larger frequencies [see Fig. 5(d)]. These states

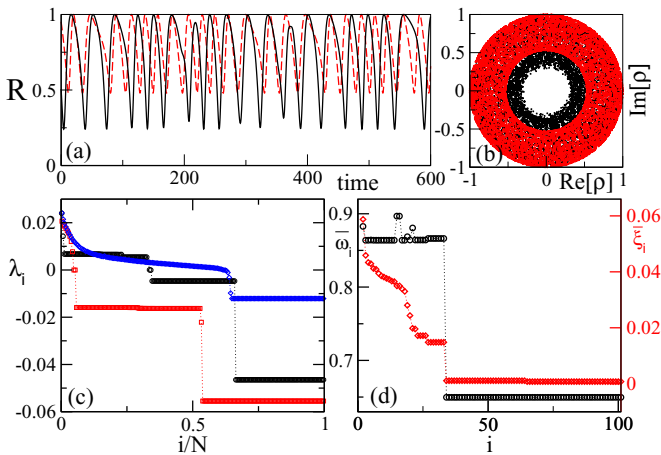


FIG. 5. (Color online) (a) Order parameters $R^{(1)}$ (black solid line) and $R^{(2)}$ (red dashed line) vs time, (b) imaginary vs real part of the complex fields $\rho^{(1)}$ and $\rho^{(2)}$, (c) Lyapunov spectra obtained for three different realizations of UCs, and (d) averaged components $\bar{\xi}_i$ (red diamonds) together with the corresponding averaged frequencies of the oscillators $\bar{\omega}_i \equiv \frac{d\theta_i}{dt}$ (black circles) for both populations. All the data refer to C2P states and to $m = 9$; the system sizes are (c) $N = 200$ and (a), (b), and (d) $N = 50$. The time averages have been performed at time $T \simeq 5 \times 10^4$.

resemble imperfect chimeras recently observed in experiments on coupled metronomes [11] and in chains of rotators [50].

The C2P states are characterized by a broken symmetry since the dynamics of the two populations takes place on different macroscopic chaotic attractors, as is clearly observable in Figs. 5(a) and 5(b). In particular, the differences in the oscillation amplitudes of $R^{(1)}$ and $R^{(2)}$ are due to the different number of oscillators contributing to the common cluster in the two populations [22,23,27]. The multistability is also reflected in the associated Lyapunov spectra. Three examples are shown in Fig. 5(c): Their shapes are extremely different, presenting different numbers of positive and negative LEs. However, a general result is that the oscillators contributing to the chaotic dynamics are the ones out of the common cluster. As shown in [46], the contribution of each oscillator i to the chaotic dynamics can be measured in terms of the corresponding squared component of the normalized maximal Lyapunov vector $\mathcal{T}^{(1)}$, namely, $\xi_i^{(\sigma)}(t) = [\delta\theta_i^{(\sigma)}(t)]^2 + [\delta\theta_i^{(\sigma)}(t)]^2$, with

$\|\mathcal{T}^{(1)}(t) = 1\|$. The time-averaged components of the vector $\bar{\xi}_i$ are shown in Fig. 5(d), where it is evident that the contribution $\bar{\xi}_i$ of the oscillators belonging to the common cluster is essentially negligible.

Conclusion. We have shown that a simple model of coupled oscillators with inertia can reproduce the erratic behaviors observed in our experiment of two coupled populations of mechanical pendulums. The presence of inertia is a distinctive ingredient to observe the emergence of chaotic regimes, such as ICCs and C2Ps. The detailed characterization of the ICC dynamics reveals that its chaotic properties can be interpreted in the framework of fully coupled dissipative systems [34]. However, our study extends the validity of the results reported in [34] to networks with inhomogeneous coupling displaying intermittent dynamics. Together with the results reported in [16,19] for a ring geometry, this clearly indicates that the stability properties of chaotic chimeras strongly depend on the underlying network topology. It would be extremely challenging to investigate if the topology also influences the stability of nonchaotic chimeras.

Our dissipative model is quite remarkable since it differs from a Hamiltonian model only by a constant dissipative term proportional to $1/m$ that vanishes in the limit of large inertia. This suggests that for sufficiently large m dynamical properties characteristic of conservative models should be observable. Indeed, the Lyapunov spectrum exhibits a pairing rule [40] similar to that of Hamiltonian models. Furthermore, ICCs are metastable states whose lifetime diverges as $\simeq N^{1.6}$, in analogy with quasistationary states in the Hamiltonian mean-field model [33].

Acknowledgments. We thank D. Angulo-Garcia, S. Lepri, O. E. Omel'chenko, A. Politi, S. Ruffo, K. A. Takeuchi, and M. Wolfrum for useful discussions and suggestions. We acknowledge partial financial support from the Italian Ministry of University and Research within the project CRISIS LAB PNR (S.O. and A.T.) and from the Human Frontier Science Program under a Cross Disciplinary Fellowship (S.T.). This work was part of the activity of the Marie Curie Initial Training Network NETT Project No. 289146 financed by the European Commission (S.O. and A.T.) and of the Dynamical Systems Interdisciplinary Network, University of Copenhagen (E.A.M.). A.T. has also been supported by the A*MIDEX grant (No. ANR-11-IDEX-0001-02) funded by the French Government “program Investissements d’Avenir”

-
- [1] Y. Kuramoto and D. Battogtokh, *Nonlinear Phen. Complex Syst.* **5**, 380 (2002).
 [2] D. M. Abrams and S. H. Strogatz, *Phys. Rev. Lett.* **93**, 174102 (2004).
 [3] D. M. Abrams, R. Mirollo, S. H. Strogatz, and D. A. Wiley, *Phys. Rev. Lett.* **101**, 084103 (2008).
 [4] S. I. Shima and Y. Kuramoto, *Phys. Rev. E* **69**, 036213 (2004).
 [5] E. A. Martens, *Phys. Rev. E* **82**, 016216 (2010).
 [6] O. E. Omel'chenko, Y. L. Maistrenko, and P. A. Tass, *Phys. Rev. Lett.* **100**, 044105 (2008).
 [7] A. Pikovsky and M. Rosenblum, *Phys. Rev. Lett.* **101**, 264103 (2008).
 [8] C. R. C. Laing, *Chaos* **19**, 013113 (2009).
 [9] S. Olmi, A. Politi, and A. Torcini, *Europhys. Lett.* **92**, 60007 (2010).
 [10] E. A. Martens, S. Thutupalli, A. Fourrière, and O. Hallatschek, *Proc. Natl. Acad. Sci. USA* **110**, 10563 (2013).
 [11] T. Kapitaniak, P. Kuzma, J. Wojewoda, K. Czolczynski, and Y. Maistrenko, *Sci. Rep.* **4**, 6379 (2014).
 [12] M. Wickramasinghe and I. Z. Kiss, *PLoS ONE* **8**, e80586 (2013).
 [13] M. R. Tinsley, S. Nkomo, and K. Showalter, *Nat. Phys.* **8**, 662 (2012).
 [14] A. M. Hagerstrom, T. E. Murphy, R. Roy, P. Hövel, I. Omelchenko, and E. Schöll, *Nat. Phys.* **8**, 658 (2012).

- [15] G. Bordyugov, A. Pikovsky, and M. Rosenblum, *Phys. Rev. E* **82**, 035205 (2010).
- [16] M. Wolfrum and O. E. Omel'chenko, *Phys. Rev. E* **84**, 015201(R) (2011).
- [17] I. Omelchenko, Y. Maistrenko, P. Hövel, and E. Schöll, *Phys. Rev. Lett.* **106**, 234102 (2011).
- [18] G. C. Sethia and A. Sen, *Phys. Rev. Lett.* **112**, 144101 (2014).
- [19] M. Wolfrum, O. E. Omel'chenko, S. Yanchuk, and Y. L. Maistrenko, *Chaos* **21**, 013112 (2011).
- [20] D. Pazó and E. Montbrío, *Phys. Rev. X* **4**, 011009 (2014).
- [21] B. Ermentrout, *J. Math. Biol.* **29**, 571 (1991).
- [22] H.-A. Tanaka, A. J. Lichtenberg, and S. Oishi, *Phys. Rev. Lett.* **78**, 2104 (1997).
- [23] H.-A. Tanaka, A. J. Lichtenberg, and S. Oishi, *Physica D* **100**, 279 (1997).
- [24] P. Ji, T. K. D. Peron, P. J. Menck, F. A. Rodrigues, and J. Kurths, *Phys. Rev. Lett.* **110**, 218701 (2013).
- [25] S. Gupta, A. Campa, and S. Ruffo, *Phys. Rev. E* **89**, 022123 (2014).
- [26] M. Komarov, S. Gupta, and A. Pikovsky, *Europhys. Lett.* **106**, 40003 (2014).
- [27] S. Olmi, A. Navas, S. Boccaletti, and A. Torcini, *Phys. Rev. E* **90**, 042905 (2014).
- [28] F. Salam, J. E. Marsden, and P. P. Varaiya, *IEEE Trans. Circuits Syst.* **31**, 673 (1984).
- [29] G. Filatrella, A. H. Nielsen, and N. F. Pedersen, *Eur. Phys. J. B* **61**, 485 (2008).
- [30] M. Rohden, A. Sorge, M. Timme, and D. Witthaut, *Phys. Rev. Lett.* **109**, 064101 (2012).
- [31] A. E. Motter, S. A. Myers, M. Anghel, and T. Nishikawa, *Nat. Phys.* **9**, 191 (2013).
- [32] B. R. Trees, V. Saranathan, and D. Stroud, *Phys. Rev. E* **71**, 016215 (2005).
- [33] A. Campa, T. Dauxois, D. Fanelli, and S. Ruffo, *Physics of Long-Range Interacting Systems* (Oxford University Press, Oxford, 2014).
- [34] K. A. Takeuchi, H. Chaté, F. Ginelli, A. Politi, and A. Torcini, *Phys. Rev. Lett.* **107**, 124101 (2011).
- [35] J. Pantaleone, *Am. J. Phys.* **70**, 992 (2002).
- [36] M. Bennett, M. F. Schatz, H. Rockwood, and K. Wiesenfeld, *Proc. R. Soc. London Ser. A* **458**, 563 (2002).
- [37] H. Ulrichs, A. Mann, and U. Parlitz, *Chaos* **19**, 043120 (2009).
- [38] E. Montbrío, J. Kurths, and B. Blasius, *Phys. Rev. E* **70**, 056125 (2004).
- [39] E. A. Martens, M. J. Panaggio, and D. M. Abrams, *arXiv:1507.01457* (2015).
- [40] The phases and frequencies are randomly chosen from the intervals $\theta_i^{(\sigma)} \in [-\pi, \pi]$ and $\dot{\theta}_i^{(\sigma)} \in [-\Omega, \Omega]$.
- [41] U. Dressler, *Phys. Rev. A* **38**, 2103 (1988).
- [42] G. Benettin, L. Galgani, A. Giorgilli, and J. M. Strelcyn, *Meccanica* **15**, 9 (1980).
- [43] M. Cencini, F. Cecconi, and A. Vulpiani, *Chaos* (World Scientific, Singapore, 2010).
- [44] O. V. Popovych, Y. L. Maistrenko, and P. A. Tass, *Phys. Rev. E* **71**, 065201(R) (2005).
- [45] J. F. Heagy, T. L. Carroll, and L. M. Pecora, *Phys. Rev. E* **52**, R1253 (1995).
- [46] F. Ginelli, K. A. Takeuchi, H. Chaté, A. Politi, and A. Torcini, *Phys. Rev. E* **84**, 066211 (2011).
- [47] The lifetime distribution, obtained for different initial conditions, is exponential, with standard deviation and average (τ) of the same order.
- [48] T. Tél and Y.-C. Lai, *Phys. Rep.* **460**, 245 (2008).
- [49] Y. Y. Yamaguchi, *Phys. Rev. E* **68**, 066210 (2003).
- [50] P. Jaros, Y. Maistrenko, and T. Kapitaniak, *Phys. Rev. E* **91**, 022907 (2015).